Y. H. Zhu[1,2], C. F. Yeung[1], W. B. Lee[1]
[1] Dept. of Manufacturing Engineering, The Hong Kong Polytechnic University, Hong Kong, China; [2] Instituto de Investigaciones en Materiales-UNAM, Mexico, Mexico

Phase Decomposition of Cast Alloy ZnAl11Cu3

Microstructure and phase transformation of a cast Zn–Al-based alloy (ZnAl11Cu3) are studied during ageing using X-ray diffraction and back-scattered scanning electron microscopy techniques. Decomposition of a zinc-rich η'_s phase is observed to take place in the way of continuous precipitation. A four-phase transformation, $\alpha + \varepsilon \rightarrow T' + \eta$, occurs during prolonged ageing. It is found that the phases involved in the phase transformation can be distinctly identified by using different atomic contrasts in the back-scattered scanning electron image of precipitates.

Keywords: Phase decomposition; Ageing; Zn–Al alloys

1 Introduction

Zinc-based alloys have been developed as one of the traditional alloys since 1922. The most popular die cast Zn-based alloy is the Zn-4 wt.% Al alloy. With small additions of Mg (about 0.03 wt.%) and Cu (up to 3 wt.%), a new family of the Zn-based alloys was developed in 1970's [1, 2]. According to the aluminum content, those commercial Zn–Al-based alloys are named ZA8, ZA12 and ZA27. In the same years, another important development of the alloys was invented in China. The chemical composition of the Zn–Al-based alloy is Zn-11 wt.% Al-3 wt.% Cu (ZnAl11Cu3). Compared with ZA12, the copper content of the alloy is higher. Because of excellent castibility and high mechanical properties, it has been extensively applied as bearing and bushing materials in many local foundries of China. One of the advantages of this structural alloy are low costs of both materials and processing, in about 50 % cost reduction compared with bronze and some Al-based alloys. However, the cast ingot of the alloy is of disadvantage in dimensional stability, such as early stage of shrinkage and expansion during prolonged ageing. For further industrial application it is important to understand the decomposition of various metastable phases in the alloy ZnAl11Cu3. Unfortunately, so far there is no publication on phase transformation and microstructural change of the alloy. The present work will study phase decomposition of this cast alloy.

2 Experimental Procedure

The test alloy was made from zinc (99.98 wt.%), aluminum (99.99 wt.%) and copper (99.99 wt.%), and melt in an induction furnace in air. The chemical composition of the alloy is Zn-Al11-Cu3Cu (wt.%). The melt was degassed by a commercial degasser, and cast at about 700 °C into a preheated sand mould. The as-cast ingots were then machined into specimens of 10 mm in diameter and 8 mm in thickness for the ageing process.

A Siemens X-ray diffractometer was used to monitor the phase transformation that occurs during ageing at 150 and 180 °C. The temperature of ageing was controlled within ±2 °C respectively. The nickel-filtered Cu K_α radiation was applied to examine the specimens after various periods of ageing with a scan speed of 1 degree per minute. The characteristic X-ray diffraction (XRD) of the alloy was collected within the diffraction angle 2θ range from 35° to 47°. Scanning electron microscopy (SEM) was employed for identifying the phases and showing the microstructural changes in the phase transformations examined. Back-scattered electron (BSE) imaging was applied to attain atomic contrast. The large atomic number differences between the aluminum-rich phase and zinc- and copper-rich phases make it possible to produce distinct images of good contrast in the alloys studied.

3 Results and Discussion

3.1 Microstructure of As-Cast Alloy ZnAl11Cu3

According to the Zn–Al phase diagram presented by Presnyakov et al. [3] a face-centered cubic (fcc) β phase solidifies firstly, when the temperature of the melt of the alloy ZnAl11Cu3 reaches the liquidus line L/β + L, as shown in Fig. 1. The β phase dissolves up to 80 wt.% Zn. Further cooling, the composition of the melt changes along the liquidus line with zinc being rejected to the melt. The β phase of richer zinc concentration subsequently solidifies outside the first solidified β phase particles to form many large (≈ 30–50 μm) and small (≈ 5–10 μm) primary β phase dendrites. Two zinc-rich hexagonal close-packed (hcp) phases: ε (Zn_4Cu) and η, solidify finally in the interdendritic regions. During solidification, the eutectic phases

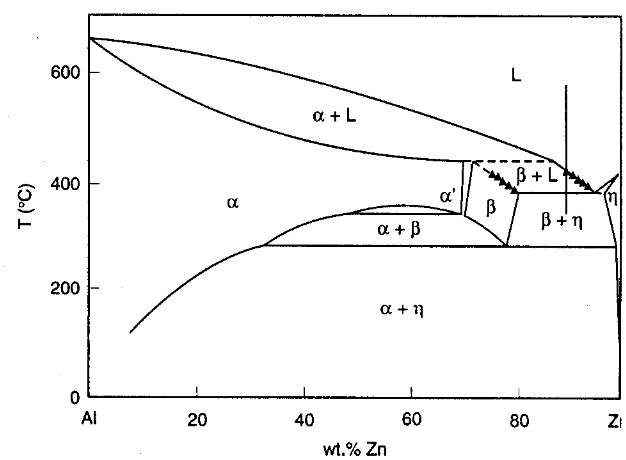

Fig. 1. Phase diagram Zn–Al [3].

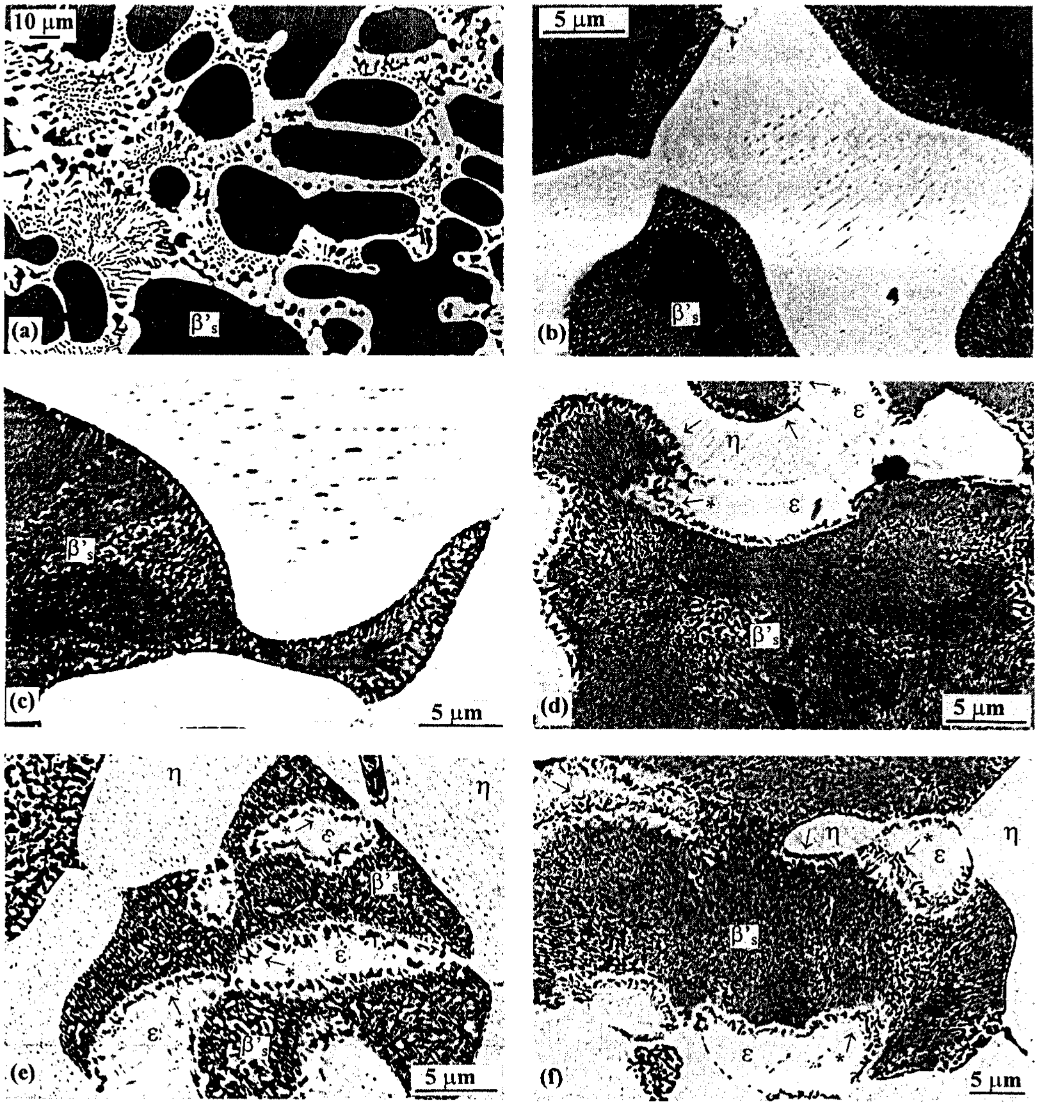

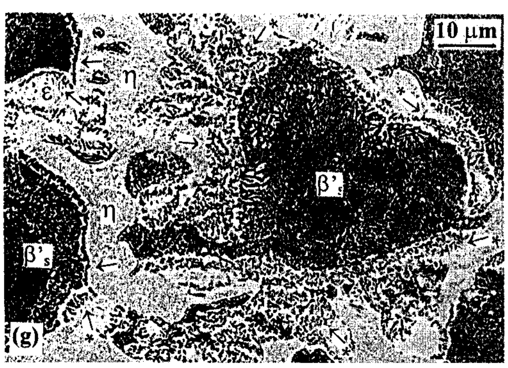

Fig. 2. Back-scattered SEM micrographs of the alloy ZnAl11Cu3: As-cast (a) and after ageing at 150 °C for 2 h (b), 8 h (c), 20 h (d), 45 h (e) 72 h (with X-ray mapping of Zn, Al and Cu) (f) and after ageing at 150 °C for 123 h and ageing at 180 °C for 6 h (g). → Dark imaged precipitates of Al rich α phase; *→ gray imaged precipitates of both Al and Cu rich T′ phase.

also form subsequently as plates or lamellae of β phase in a matrix of zinc-rich η and ε phases, as shown in Fig. 2a. The interlamellar spacing is about 3–5 μm.

During cooling after solidification, these three phases, β, η and ε, become various supersaturated phases, β'_s, η'_s and ε. It was reported that the β'_s phase decomposed into three phases in a cellular reaction: $\beta'_s \rightarrow \alpha + \eta + \varepsilon$, where the α phase is a fcc Al-rich phase [4, 5]. There are only three phases in the as-cast alloy: supersaturated η'_s, α and ε, as shown in X-ray diffractograms (Figs. 3 and 4).)

No XRD of the β'_s phase exists. During cooling after casting, various Zn-rich η'_s phases form together with the new-formed η phase derived from decomposition of the β'_s phase. Accordingly, multi-overlapped (0002) diffraction peaks of the Zn-rich η'_s phase are observed at $2\theta \approx 36.4$ and 36.6° in the as-cast alloy, as shown in Figs. 3 and 4.

3.2 Decomposition of the β'_s, Zn-rich η'_s and ε Phases

Further decomposition of the β'_s phase is observed in the cast alloy during ageing. A coarse lamellar structure forms in the outer layer of the β'_s phase dendrites, whilst the inner part appears as fine lamella, as shown in Fig. 2b. It is because the outer layer contains more zinc. As reported in previous studies [6, 7], Zn atoms diffuse more rapidly than Al atoms, which results in faster decomposition of the β'_s phase.

The decomposition of the Zn-rich η'_s phase occurs also during ageing. As shown in the X-ray diffractograms of the alloy aged at 180 °C (Fig. 3), the multi-overlapped (0002) diffraction peaks of the η'_s phase shifts to a lower 2θ value (36.6°) as a single metastable η phase after ageing at 180 °C for 15 min, accordingly the *d* spacing decreases to 0.2453 nm. This stage of decomposition of the η'_s phase is observed in more detail in the specimen aged at 150 °C, as shown in Fig. 4. The multi-overlapped (0002) diffraction peaks of the η'_s phase shift to 36.6° after ageing at 150 °C for 30 min. Further ageing at both 180 and 150 °C, the decomposition of the metastable Zn-rich η phase is observed. The (0002) X-ray diffraction peak shifts gradually to lower 2θ value, accordingly the *d* spacing of the (0002) planes increases gradually to 0.2463 μm after ageing at 180 °C for 42 h, and to 0.2467 nm after ageing at 150 °C for 262 h, as indicated in Figs. 3 and 4. In most cases, the XRD angles of the $(10\bar{1}0)$ and $(10\bar{1}1)$ planes of the Zn-rich η phase remain at about 39.1° and 43.3°, respectively, with *d* spacings of 0.2302 and 0.2084 nm accordingly. These appear as characteristics of the decomposition of the Zn-rich η phase.

The continuous precipitation is clearly seen in the BSE image, as shown in Figs. 2b and c. Compared with the precipitates after ageing at 150 °C for 2 h, the dark imaged Al-rich precipitates have developed and grown directionally after ageing at 150 °C for 8 h inside the light contrast Zn-rich η phase. It is interesting to find that this is different from the decomposition of the zinc-rich η'_s and η phases in the aged eutectoid Zn–Al-based alloy (ZnAl22Cu3) after various thermal and thermo-mechanical processes, such as cast, extrusion, and furnace cooling. The latter occurred at

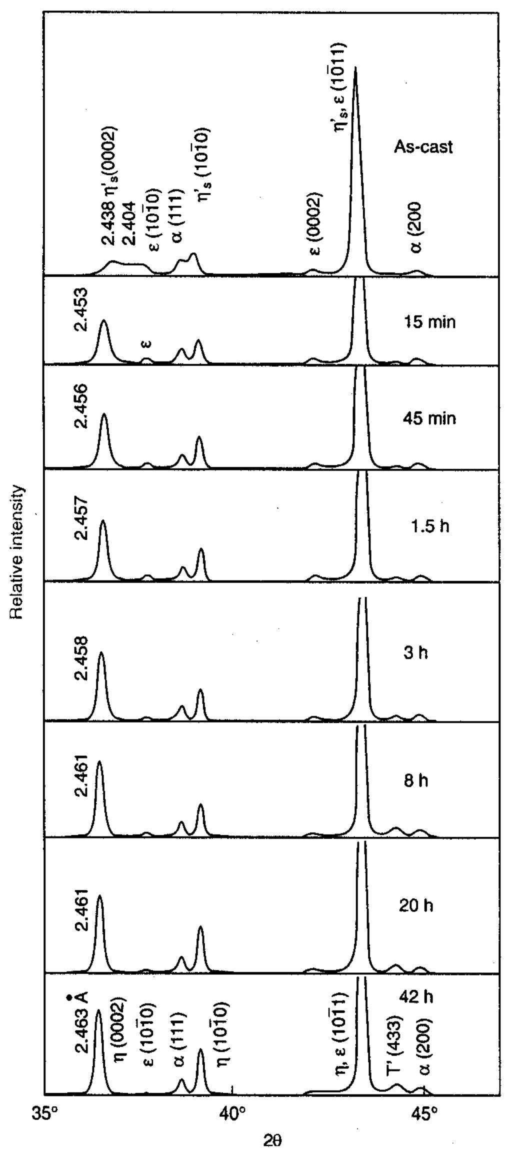

Fig. 3. X-ray diffractograms of the as-cast alloy and after various stages of ageing at 180 °C.

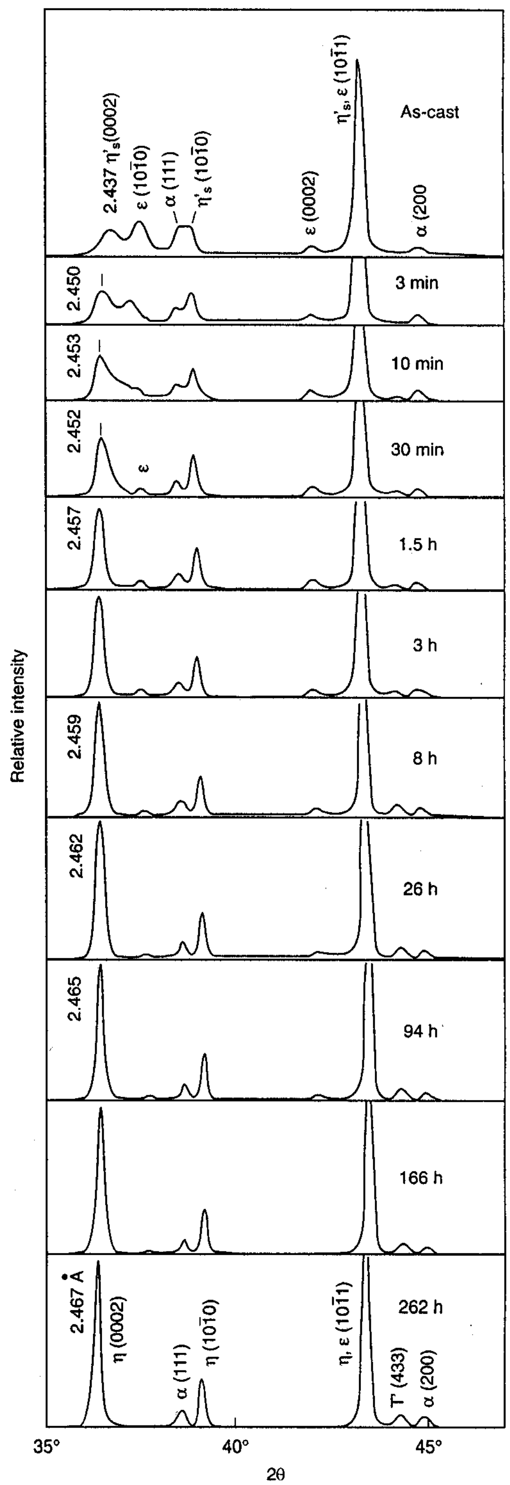

Fig. 4. X-ray diffractograms of the as-cast alloy and after various stages of ageing at 150 °C.

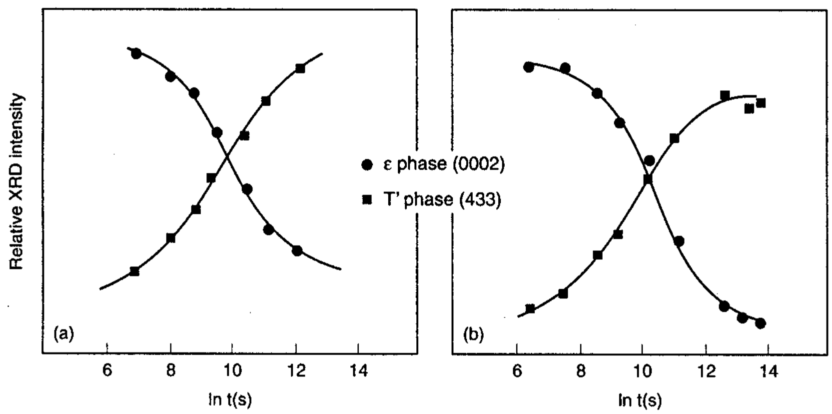

Fig. 5. Relative XRD intensity changes of the ε and T′ phases in the cast alloy aged at 180 °C (a) and 150 °C (b).

the grain boundaries and phase boundaries as discontinuous precipitation [8–10].

During prolonged ageing, the decomposition of the ε phase occurs in the cast alloy. As shown in Fig. 3, the X-ray diffraction intensities of the ε phase both at the $(10\bar{1}0)$ and (0002) planes decrease during prolonged ageing, accompanying increase in the X-ray diffraction intensity of the (433) peak of the T′ phase. The intensities of the $(10\bar{1}0)$ and (0002) peaks have considerably decreased after ageing at 180 °C for 20 h, and 94 h, respectively, while the (433) peak of the T′ phase has greatly increased. The ε phase vanishes finally. The relative XRD intensity changes of the ε and T′ phases are obtained by calculating the area covered by the related characteristic diffraction peaks, and then plotted against ln *t* (here, *t* is the ageing time in seconds) for the cast alloy aged at 180 and 150 °C, as shown in Fig. 5. This has been well recognized as a four-phase transformation: $\alpha + \varepsilon \rightarrow T' + \eta$, which occurs in the Zn–Al-based alloys during prolonged stages of various thermal or thermo-mechanical processes [4–14].

By using atomic contrast in the BSE image, the decomposition of the ε phase is clearly observed. After ageing at 150 °C for 20 h, gray imaged precipitates of the Cu- and Al-rich T′ phase are observed at the phase boundaries of the light contrast ε phase and the decomposed β_s' phase, as indicated by arrows (*→) in Fig. 2d. Obviously, the ε phase reacts with the α phase, one of the three decomposition products of the β_s' phase, i. e., $\beta_s' \rightarrow \alpha + \eta + \varepsilon$. This gray precipitate does not appear at the phase boundaries of η and the decomposed β_s' phase. Dark imaged Al-rich α phase remains unchanged at this part of the decomposed β_s' phase boundaries, as indicated by arrows (→) in Fig. 2d. The phase boundaries of the η and ε phases of light contrast are clearly distinguished from each other by a distinct contrast between the gray T′ phase precipitates and the dark α phase precipitates, as shown in Fig. 2d. After ageing at 150 °C for 45 h, the decomposition of the ε phase has developed, and the ε phase particles are clearly observed (Fig. 2e).

Fig. 2f is a BSE image of the alloy specimen after ageing at 150 °C for 72 h. It was clearly observed that the ε phase particles with gray precipitates of the T′ phase indicated by (*→) gives a brighter Cu K_α X-ray mapping than the decomposed β_s' phase and the η phase. It is because there is less Cu in both of the decomposed β_s' phase and the η phase than in the ε phase. The X-ray mapping results are in good agreement with the above mentioned identification of phases by using different contrasts of the precipitates.

After ageing at 150 °C for 123 h and ageing at 180 °C for 6 h, the T′ phase precipitates are considerably developed, which implies that the ε phase has mostly decomposed in the way of the four-phase transformation: $\alpha + \varepsilon \rightarrow T' + \eta$ (Fig. 2g).

4 Conclusions

1. The microstructure of the as-cast alloy ZnAl11Cu3 consists of many large (≈30–50 μm) and small (≈5–10 μm) primary β phase dendrites in a lamellar eutectic matrix of β phase and Zn-rich η and ε phases.
2. During ageing the decomposition of the Zn-rich η_s' phase occurs by continuous precipitation.
3. Decomposition of the ε phase takes place via a four-phase transformation: $\alpha + \varepsilon \rightarrow T' + \eta$, during prolonged ageing.
4. The phase boundaries of the η and ε phases can be clearly distinguished from each other by a distinct contrast between the gray T′ phase precipitates and the dark α phase precipitates.

The authors would like to express their thanks to M. N. Yeung, L. Banos, A. Caballero and P. S. L. Chan for their assistance in the experimental work, and also to The Research Committee of The Hong Kong Polytechnic University (Project No. GYY11) and DGAPA de UNAM (Project No. IN503797) for their financial supports.

References

1. Gervais, E.; Levert, H.; Bess, M.: AFS Trans. 88 (1980) 183.
2. Barnhurst, R.J.; Gervais, E.; Beyes, F.D.: AFS Trans. 91 (1983) 569.
3. Presnyakov, A.A.; Goltban, Y.A.; Cherpyakova, V.V.: Russ. J. Phys. Chem. 35 (1961) 623.
4. Zhu, Y.H.; Murphy, S.: Chin. J. Mater. Sci. & Technol. 3 (1987) 261.
5. Zhu, Y.H.: Chin. J. Mater. Sci. & Technol. 6 (1990) 125.
6. Ciach, R.; Duliet-Zawedzka, B.; Ciach, T.D.: J. Mater. Sci. 13 (1978) 2676.
7. Kleschev, G.V.; Yelistrator, A.M.; Seynkman, A.I.: Fiz.Tverd Tel. 9 (1967) 2811.
8. Zhu, Y.H.; Man, H.C.; Dorantes Rosales, H.J.; Hernandez Flores, R.M., in: A.M. Hamouda, S. Sulaiman, M. Ahmadun, (eds) Proc. Int. Conf. on Advances in Materials Processing and Technologies, Malaysia, 1 (1998) 89.
9. Zhu, Y.H.: J. Mater. Res. 11 (1996) 593.
10. Zhu, Y.H.: J. Mater. Sci. Lett. 15 (1996) 1888.
11. Zhu, Y.H.; Hernandez Flores, R.M.; Banos, L.: J. Mater. Sci. 34 (1999) 1.
12. Ciach, R.; Krol, J.; Wegrzyn-Tasio, K.: Bull. Acad. Polon. Sci. (Technol.) 17 (1969) 371.
13. Krol, J.; Wegrzyn, K.: Arch. Hutn. 16 (1971) 119.
14. Murphy, S.: Z. Metallkd. 71 (1980) 96.

(Received October 9, 2000)

Correspondence Address

Dr. Y. H. Zhu
IIM, UNAM
Apartado Postal 70-360, Mexico D.F. 04510, Mexico
Fax: +52 5616 1371
E-mail: yaohuazhu@hotmail.com